Multi-year monitoring of rift propagation on the Amery Ice Shelf, East Antarctica

H. A. Fricker,[1] N. W. Young,[2] R. Coleman,[3] J. N. Bassis,[1] and J.-B. Minster[1]

Received 16 July 2004; revised 18 October 2004; accepted 11 November 2004; published 21 January 2005.

[1] We use satellite imagery from four sensors (Multi-angle Imaging SpectroRadiometer (MISR), Enhanced Thematic Mapper (ETM), and RADARSAT and ERS Synthetic Aperture Radar (SAR) to monitor the lengths of two rifts on the Amery Ice Shelf, from 1996 to 2004. We find that the rifts have each been propagating at a steady annual rate for the past 5 years. Superimposed on this steady rate is a seasonal signal, where propagation rates are significantly higher in the summer period (i.e., September–April) than in the winter period (i.e., April–September). Possible causes of this summer-winter effect are changing properties of the ice mélange, which fills the rifts, and seasonal changes in ocean circulation beneath the ice shelf. **Citation:** Fricker, H. A., N. W. Young, R. Coleman, J. N. Bassis, and J.-B. Minster (2005), Multi-year monitoring of rift propagation on the Amery Ice Shelf, East Antarctica, *Geophys. Res. Lett.*, *32*, L02502, doi:10.1029/2004GL021036.

1. Introduction

[2] Iceberg calving and basal melting from ice shelves redistribute the majority of the ice flux from the grounded Antarctic ice sheet into the Southern Ocean [*Jacobs et al.*, 1992]. Because of their direct contact with the ocean and their sensitivity to air temperature warming, it is likely that the first signs of change in the Antarctic ice sheet will be seen in the ice shelves [*Mercer*, 1978; *Doake and Vaughan*, 1991], making them sensitive indicators of climate change. Indeed, several ice shelves of the Antarctic Peninsula have receded over the past several decades, and more recently have exhibited dramatic breakup over periods as short as several days [*Doake and Vaughan*, 1991; *Rott et al.*, 1996]. Although the large ice shelves (Ross, Filchner-Ronne and Amery) are not currently showing any signs of peninsular-style disintegration, they do all advance and retreat as part of their natural cycle. The Amery Ice Shelf (AIS) is further north than Ross and Filchner-Ronne ice shelves, and it has been suggested that it may be susceptible to breakup within a few decades if it experiences warming trends similar to those which took place on the Peninsula [*Scambos et al.*, 2003].

[3] Tabular iceberg calving events are sporadic with typical recurrence intervals of several decades and more [*Budd*, 1966; *Jacobs et al.*, 1986]. In order to evaluate realistically the evolution of ice shelves under different climate change scenarios, we need to determine how these scenarios might influence the production rate of icebergs. A precursor to calving is the initiation and subsequent propagation of rifts which penetrate the entire ice shelf thickness. Such "through-cutting" rifts propagate and widen, until they eventually become detachment boundaries for tabular bergs. Despite the important role of rift formation and propagation in the calving process, we know very little about the mechanisms involved. This ignorance highlights a need to describe and incorporate fracture mechanics properly into models of ice shelf dynamics [*Rist et al.*, 2002; *Hammann and Sandhager*, 2005].

[4] AIS is the largest ice shelf in East Antarctica. Its last major calving event occurred in the 1963–64 summer, which released a giant tabular iceberg about 10 000 km^2 [*Budd*, 1966]. Since then it has only produced small icebergs, but a rift system has been evolving at the front for the past two decades (Figure 1). Here we describe the evolution of this rift system over eight years (1996–2004), by measuring rift lengths in satellite imagery.

2. Loose Tooth Rift System

[5] At the present time, the rift system at the center of the AIS front consists of four rifts: two longitudinal (parallel-to-flow) ~25 km apart (L1 and L2), and two transverse-to-flow (T1 and T2) (Figure 1). It outlines an area of ice that has been colloquially named the "Loose Tooth", and we refer to it here as the LT rift system. L1 and L2 initiated in the early 1980's within the boundaries of adjacent flowbands, formed where ice streams merged together hundreds of kilometers upstream. L1 and L2 formed between these flowbands at the ice front as the ice shelf protruded beyond the confines of its embayment and spread laterally. The longitudinal rifts then propagated upstream along the flowband boundaries. L1 stopped propagating in the mid 1990's when it was 23 km in length and branched, forming a triple junction, and spawning rifts T1 and T2. Around the same time L2 stopped propagating. The L1/T1/T2 triple junction remains a prominent feature of the LT rift system, and T1 and T2 are both active. GPS and seismic measurements collected at the tip of T2 during the 2002/03 austral summer indicate this rift propagates episodically in a series of rupture events (J. N. Bassis et al., Propagation of an active rift in the Amery Ice Shelf, East Antarctica, submitted to *Geophysical Research Letters*, 2004, hereinafter referred to as Bassis et al., submitted manuscript, 2004).

[6] The propagation of T2 will ultimately result in the release of a ~30 km × 30 km iceberg i.e., when T2

[1]Institute of Geophysics and Planetary Physics, Scripps Institution of Oceanography, La Jolla, California, USA.
[2]Department of the Environment and Heritage, Australian Antarctic Division and Antarctic Climate and Ecosystems Cooperative Research Centre, Hobart, Tasmania, Australia.
[3]School of Geography and Environmental Studies, University of Tasmania and Antarctic Climate and Ecosystems Cooperative Research Centre, Hobart, Tasmania, Australia.

0094-8276/05/2004GL021036$05.00

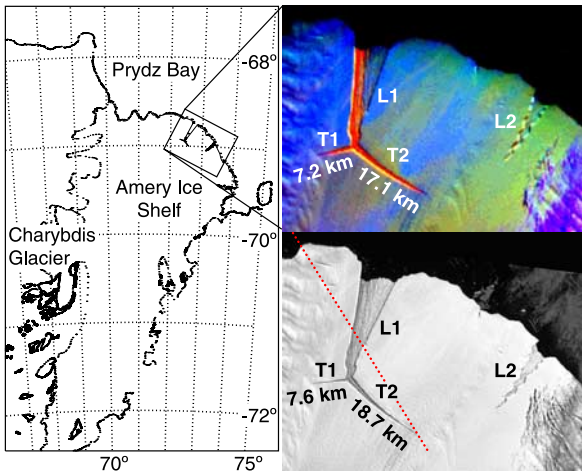

Figure 1. Top panel: Map showing location of AIS rift system. Middle and bottom panels: MISR (TERRA) and ETM (Landsat-7) images over rift system, acquired 2 March 2003. TERRA and Landsat-7 follow the same ground track, ~20 minutes apart. MISR image is a false-color composite of the red bands from the CF, AN and CA cameras, in which color acts as a proxy for angular reflectance variations which are related to surface texture, and enhances the rifts. ETM image is Band 4. Length estimates for rifts are shown for each image, which are different due to image resolution (see Figure 2 caption). Location of Figure 3 profile is indicated as a red dashed line.

connects L1 with L2. An embayment of this size was seen in the AIS front in a 1962 satellite image, indicating that a similar calving event also took place during the last calving cycle [*Fricker et al.*, 2002].

3. Data and Method

[7] We gathered all the available imagery over the LT rift system from 1996 to 2004 from MISR (TERRA), ETM (Landsat-7), ERS SAR and RADARSAT SAR. We selected 75 clear MISR images acquired between March 2000 and April 2004 (Paths 125–130), 5 ETM images (February 2000, January and December 2001, November 2002 and March 2003), ERS SAR from March 1996, and various RADARSAT ScanSAR images from 1997 and 2000. Example MISR and ETM images are shown in Figure 1. Each image was contrast-stretched to enhance the rifts, and rift lengths were estimated along the upstream rift wall, from the "v" in the triple junction to the rift tips. Note that what we measure is the trace of the rift, i.e., the surface expression. For each image the rift length estimate is to the point on the image where it occupies enough of the pixel to contrast against the background.

[8] No ETM or MISR images are available from April through September due to the lack of sunlight at the time of the overpass. We shall refer to this blackout period as "winter" to distinguish it from our "summer" which lasts from September through April. During the period covered by MISR the average sampling time between clear images is about 14.5 days.

4. Results

[9] The eight-year time series compiled from the different sensors show an overall increase in the lengths of both rifts (Figure 2a). Between March 1996 and April 2004, T1 lengthened from 0.9 to 8.1 km and T2 grew from 2.8 to 18.0 km. Over the second half of each time series, MISR provides dense temporal sampling during summers: the latter part of 1999/00 (4 clear images) and all of 2000/01 to 2003/04 (13, 20, 14 and 19 clear images respectively). MISR length estimates are in broad agreement with those obtained from other instruments, although the lower spatial resolution of MISR *vs.* ETM means that the position of the rift tip is harder to detect in MISR, resulting in rift length estimates that are generally ~1 km shorter (Figures 1 and 2). An exception was 7 January 2001, when the ETM image was acquired on an ascending pass with low light levels. Conversely, MISR lengths are generally longer than those from RADARSAT ScanSAR, by ~1 km. This is because ScanSAR images were acquired along a descending orbit, and the radar look angle is approximately parallel to the rift axis. This leads to low backscatter from the rift and, therefore, lower contrast with respect to the surrounding ice shelf.

[10] MISR rift length estimates show seasonal variation superimposed on the multi-year linear trend (Figure 2b). In general, rift lengths at the beginning of a summer are similar to those at the end of the previous summer, indicating that

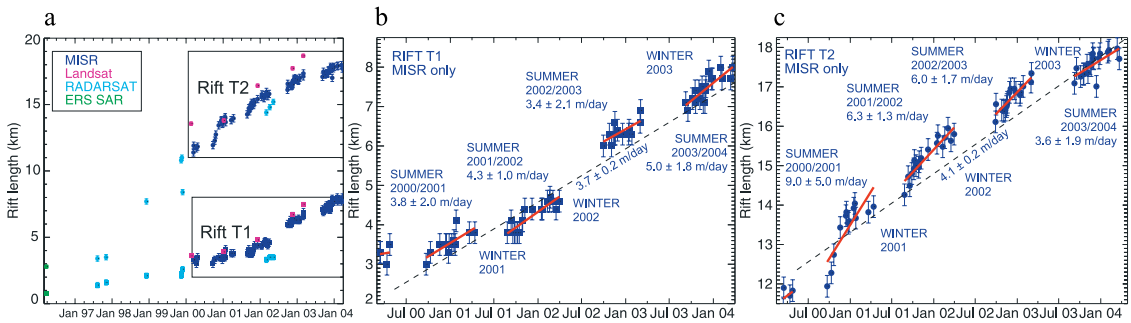

Figure 2. (a) Measured rift lengths derived from satellite imagery from 1996 to present. For each image type, the error bars represent 1 pixel, where the pixel sizes are: ETM = 12.5 m; ERS = 100 m; RADARSAT = 200 m; MISR = 275 m. (b–c) MISR time series for T1 and T2, showing results of regression analysis given in Table 1 (red solid lines are Case A and black dashed line is Case C).

Table 1. Propagation Rates and 95% Confidence Intervals (in m day^{-1}) Derived From the MISR Time Series Using Three Centered Regression Analysis Cases

		T1		T2	
Case[a]		Rate	CI	Rate	CI
A	1999/2000	2.6	32.7	4.4	31.2
	2000/2001	3.8	2.0	9.0	5.0
	2001/2002	4.3	1.0	6.2	1.3
	2002/2003	3.4	2.1	6.0	1.7
	2003/2004	5.0	1.8	3.6	1.9
B		3.7	0.2	4.1	0.2
C		4.3	0.7	6.1	1.1

[a]A: individual summers B: full five-year time series and C: common slope which gives an ''average summer'' rate.

the rifts have not lengthened significantly over winter. An exception to this pattern is winter 2002, when T1 grew significantly. We perform a centered regression analysis for three different cases using the MISR rift lengths (Table 1 and Figure 2). For Case A, separate linear trends are made for both rifts to each summer. Case B is a linear trend to all data, relative to 1 July 1999, giving the multi-year trend. Case C, the third regression model, represents an ''average summer'' rate, where a single (common) slope is determined for all of the summers, together with intercepts for each season.

[11] Case A solutions (Table 1), suggest that the propagation rates are increasing for T1 and decreasing for T2. Using pairwise t-tests, we find that the slopes for individual summer seasons are not statistically different from each other at the 95% CI, but continued monitoring is required to determine whether this is indeed true. There is some evidence of rate change as the summer season progresses (Figure 2), indicating an apparent slowing down of the propagation rate over the summer, although the data are noisy. The best example of this is T2 in summer 2002/03. Given the noise, and the length and sampling interval of our current time series, it is difficult to say whether this is a real signal. We considered that it might be a result of changing solar angle over summer; however, the data noise precluded us from finding a meaningful correlation between rift length and solar angle. More in situ measurements would help resolve this issue.

[12] Slopes for individual summer seasons (Case A) are generally higher than the multi-year slope (Case B), implying that there is a lower rate over winter. To test this we first compare regression slopes with a pairwise t-test, which indicates that at the 95% confidence level there is some evidence that the slopes of the lines differ, especially for seasons 2001/02 and 2002/03 for T2. However, since all of our rift length measurements are from summer, we cannot determine winter propagation rates nor the time period when the rates change. Instead, we can only examine the rift behavior during the summer and use the results to infer an average behavior during the winter. Visually (Figure 2b), the winter rates appear lower than the summer rates. To investigate this further and to determine if there is a seasonal difference we compare the propagation rates for Cases A and C against those from Case B with a likelihood ratio test. The results confirm that the winter rates are statistically different from the summer rates. The best way to verify this seasonal pattern would be to have field instrumentation deployed for a full year or to acquire imagery during winter.

5. Discussion

[13] Our results indicate that the propagation rates of rifts T1 and T2 have been steady (within data noise) over the eight ''summer'' years of satellite observation (1996–2004), and thus have both been active since their initiation around 1995. However, we have observed a significant seasonal variability in propagation rates (Figure 2b): rates are generally higher in the summer and lower in the winter. An exception is winter 2002 when T1 grew significantly. We suggest that this is due to T1 meeting the Charybdis Glacier flowband (Figure 1), which has different ice properties to the adjacent flowband, and contains km-scale crevasses at its eastern edge (visible in a high resolution ETM image, Path 038 Row 135 7 Jan 2001). T1 may have intersected with one of these crevasses causing an apparent jump in rift length from 4.7 to 6.1 km.

[14] The observed seasonal pattern was initially thought to be an observational effect due to slumping of snow bridges at the start of summer. However, because of the large pixel size of MISR (275 m), we do not resolve the exact location of the rift tip, and at the point on the rift which we detect, we estimate that it is already too wide to support a snow bridge. From the ETM image (Figure 2), T2 is ~40 m wide just 1 km from the rift tip. Furthermore, T2 is growing at 4–8 m day^{-1}, and it is unlikely that such an active rift could support snow bridges in the long-term. Ground penetrating radar observations made across a shear zone on Ross Ice Shelf showed that the widest snow-bridge-covered rifts encountered were 10 m [*Delaney et al.*, 2004]. At the T2 tip, Bassis et al. (submitted manuscript, 2004) noted that snow bridges present in early December had slumped by late January. This occurs later in the season than the onset of higher propagation rates. The combination of these factors leads us to reject the notion that our observations are linked to snow bridges.

[15] I. Joughin and D. R. MacAyeal (Calving of large tabular icebergs from ice-shelf rift systems, submitted to *Geophysical Research Letters*, 2004) suggest that background glaciological stress is the primary driving force in rift widening, however this is unlikely to be susceptible to seasonal variations. Changes in external environmental variables, such as ocean swell, ocean circulation, sea-ice or fast-ice concentration, winds, storms and tides might affect rift propagation rates. Ocean mooring data from 2001 at a depth of 370 m near the L1 mouth shows cold Ice Shelf Water exiting the sub-ice-shelf cavity between April and mid-August (H. Leffanue et al., The seasonality of water masses and circulation at the Amery Ice Shelf, manuscript in preparation, 2004, hereinafter referred to as Leffanue et al., manuscript in preparation, 2004) and warmer Shelf Waters flowing into the cavity from September. Since rifts introduce a discontinuity in the water column thickness, it seems likely that the rift has an effect on the ice-ocean interaction there. Ocean circulation beneath the ice shelf will generate drag on the underside of the shelf causing varying stresses on the rifts, but this is difficult to estimate quantitatively without a detailed modeling study. It does appear, however, that the timing of the circulation changes

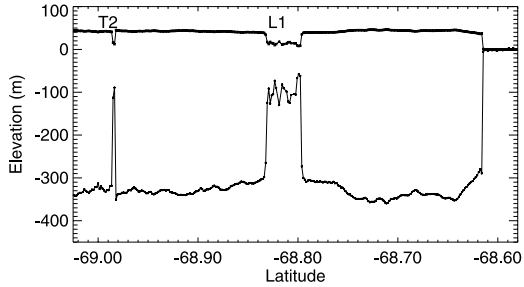

Figure 3. GLAS elevation profile across T2 and L1 (ground-track shown in Figure 1) with bottom profile derived from the hydrostatic relationship assuming the following column-averaged densities: 1028 kg m^{-3} for sea-water, 876 kg m^{-3} for ice shelf ice and 865 kg m^{-3} for mélange [*King*, 1994].

correlates closely with the changes in rift propagation rates. In the winter, ocean swell is damped by sea-ice cover in Prydz Bay. If ocean swell was a controlling factor, we would expect that the onset of a higher rate of propagation would be related to a reduction in sea-ice concentration. However, maximum sea-ice concentration occurs in October [*Jacka*, 1983] when propagation rates are already high. Bassis et al. (submitted manuscript, 2004) concluded that environmental forcings were unlikely to control propagation rates but were unable to rule out a link between winds and propagation events seen in GPS data. However, such a putative link would be more consistent with faster rift propagation during the winter, when winds are strongest, the opposite of what we observe. Similarly, storms are more frequent in winter, so we do not think these effects are controlling factors.

[16] Another component of the ice rift system which we consider might change on a seasonal basis is ice *mélange,* a mixture of sea-ice, accumulated and wind-blown snow, ice fragments broken off the ice shelf and marine ice, which fills the rifts [*MacAyeal et al.*, 1998; *Khazendar and Jenkins*, 2003]. *Larour et al.* [2004] suggested that mélange thickness may exert a control on rift propagation, i.e., thick mélange slows propagation. These authors also show evidence of higher propagation rates in summer. Data from the Geoscience Laser Altimeter System (GLAS) on NASA's Ice, Cloud and land Elevation Satellite (ICESat) provide an estimate of the mélange thickness. A profile across rift T2 (Figure 3) on 18 October 2004 shows that the ice mélange was 87.2 ± 14.3 m thick, accounting for around one third of the ice shelf thickness. There is no evidence of a seasonal change in mélange thickness. The observed seasonal changes in rift growth rates might be due to changes in mélange properties throughout the year. From field observations we expect that a large fraction of the mélange column thickness comes from ice blocks that fall from the rift walls as the rift widens. In the winter, cold sea-water intrusions from below might bind these ice blocks together, giving the mélange more mechanical strength and slowing rift propagation. Conversely in summer when the intruding water is warmer (Leffanue et al., manuscript in preparation, 2004), the mélange might decrease in strength, leading to faster rift propagation. The remainder of the mélange column derives from the processes of sea-ice and marine ice formation, and snow accumulation which vary on different time scales, and produce ice with different properties; the net effect of these processes acting together is a mélange ice column that may have a complicated seasonal behavior. Our results point to a need to look more closely at this unique ice blend, as it is potentially important in controlling iceberg calving rates, and therefore in determining the stability of an ice shelf.

6. Conclusions

[17] We have measured the growth of two active rifts at the front of the AIS using a combination of satellite imagery, indicating steady multi-year propagation rates for the past 5 years. However, there appears to be a seasonal dependence: rifts generally propagate faster in the summer than in the winter. We suggest that the seasonal pattern may be a result of changing properties of ice mélange inside the rift throughout the year and/or ocean circulation changes beneath the ice shelf. The seasonal dependence of rift propagation rates is an intriguing result which contradicts the current assumption that the calving of large tabular bergs is insensitive to seasonal effects. Our results emphasize the need for long-term year-round monitoring of ice shelf processes.

[18] **Acknowledgments.** We thank C Averill and D Diner for help with the MISR images. MISR data were provided by the Langley Data Center. ERS/RADARSAT SAR data were provided by the Alaska SAR Facility through NASA grant NAG5-10065. L-7 ETM data obtained through LP-DAAC at USGS, with special assistance from J Dwyer. GLAS data were acquired through NASA contract NAS5-99006. Work at SIO supported by NAG5-10065, NAS5-99006 and NSF grant OPP-0337838. RC and NY supported by the Australian Government's Cooperative Research Centres Programme through the ACE-CRC. We thank the Editor, T Scambos, an anonymous reviewer and R Warner for their helpful comments.

References

Budd, W. (1966), The dynamics of the Amery Ice Shelf, *J. Glaciol.*, *6*, 335–358.

Delaney, A., S. A. Arcone, A. O'Bannon, and J. Wright (2004), Crevasse detection with GPR across the Ross Ice Shelf, Antarctica, paper presented at 10th International Conference on GPR, Delft, Netherlands, 21–24 June.

Doake, C. S. M., and D. G. Vaughan (1991), Rapid disintegration of the Wordie Ice Shelf in response to atmospheric warming, *Nature*, *350*, 328–330.

Fricker, H. A., N. Young, I. Allison, and R. Coleman (2002), Iceberg calving from the Amery Ice Shelf, East Antarctica, *Ann. Glaciol.*, *34*, 241–246.

Hammann, A., and H. Sandhager (2005), Propagation of cracks through an ice shelf as precondition for calving: Numerical experiments with an idealised glacial system, in *Forum for Research on Ice Shelf Processes*, *FRISP Rep. 14*, edited by H. Oerter, Alfred Wegener Inst., Bremerhaven, Germany, in press.

Jacka, T. H. (1983), A computer data base for Antarctic sea ice extent, *ANARE Res. Notes 13*, 54 pp., Aust. Natl. Antarct. Res. Exped., Melbourne, Victoria, Australia.

Jacobs, S. S., D. R. MacAyeal, and J. L. Ardai Jr. (1986), The recent advance of the Ross Ice Shelf, Antarctica, *J. Glaciol.*, *32*, 464–474.

Jacobs, S. S., H. Helmer, C. S. M. Doake, A. Jenkins, and R. M. Frolich (1992), Melting of the ice shelves and the mass balance of Antarctica, *J. Glaciol.*, *38*, 375–387.

Khazendar, A., and A. Jenkins (2003), A model of marine ice formation within Antarctic ice shelf rifts, *J. Geophys. Res.*, *108*(C7), 3235, doi:10.1029/2002JC001673.

King, E. C. (1994), Observations of a rift in the Ronne Ice Shelf, Antarctica, *J. Glaciol.*, *40*, 187–189.

Larour, E., E. Rignot, and D. Aubry (2004), Modelling of rift propagation on Ronne Ice Shelf, Antarctica, and sensitivity to climate change, *Geophys. Res. Lett.*, *31*, L16404, doi:10.1029/2004GL020077.

MacAyeal, D. R., E. Rignot, and C. Hulbe (1998), Ice shelf dynamics near the front of the Filchner Ronne Ice Shelf, East Antarctica, revealed by SAR interferometry: Model/interferogram comparison, *J. Glaciol.*, *44*, 419–428.

Mercer, J. H. (1978), West Antarctic ice sheet and CO_2 greenhouse effect: A threat of disaster, *Nature*, *271*, 321–325.

Rist, M. A., P. R. Sammonds, H. Oerter, and C. S. M. Doake (2002), Fracture of Antarctic shelf ice, *J. Geophys. Res.*, *107*(B1), 2002, doi:10.1029/2000JB000058.

Rott, H., P. Skvarca, and T. Nagler (1996), Rapid collapse of northern Larsen Ice Shelf, Antarctica, *Science*, *271*, 788–792.

Scambos, T., C. Hulbe, and M. Fahnestock (2003), Climate-induced ice shelf disintegration in the Antarctic Peninsula, in *Antarctic Peninsula Climate Variability: Historical and Paleoenvironmental Perspectives*, *Antarct. Res. Ser*, vol. 79, edited by E. Domack et al., pp. 79–92, AGU, Washington, D.C.

H. A. Fricker, J. N. Bassis, and J.-B. Minster, Institute of Geophysics and Planetary Physics, Scripps Institution of Oceanography, 9500 Gilman Dr., La Jolla, CA 92093, USA. (hafricker@ucsd.edu)

R. Coleman, School of Geography and Environmental Studies, University of Tasmania and Antarctic Climate and Ecosystems Cooperative Research Centre, Private Bag 78, Hobart, Tas 7001, Australia.

N. W. Young, Department of the Environment and Heritage, Australian Antarctic Division and Antarctic Climate and Ecosystems Cooperative Research Centre, Private Bag 80, Hobart, Tas 7001, Australia.